Bioorg. Med. Chem. Lett. 42 (2021) 127999

Contents lists available at ScienceDirect

Bioorganic & Medicinal Chemistry Letters

journal homepage: www.elsevier.com/locate/bmcl

Design, synthesis and *in-vitro* evaluation of fluorinated triazoles as multi-target directed ligands for Alzheimer disease

Dalvi Tanay[a,d], Dewangan Bhaskar[a,d], Agarwal Gopal[b,d], Shinde Suchita Dattatray[a], Jain Alok[b,e], Srivastava Akshay[c], Sahu Bichismita[a,*]

[a] Department of Medicinal Chemistry, National Institute of Pharmaceutical Education and Research (NIPER) Ahmedabad, Opposite Air Force Station, Palaj, Gandhinagar, Gujarat 382355, India

[b] Department of Biotechnology, National Institute of Pharmaceutical Education and Research (NIPER) Ahmedabad, Opposite Air Force Station, Palaj, Gandhinagar, Gujarat 382355, India

[c] Department of Medical Devices, National Institute of Pharmaceutical Education and Research(NIPER) Ahmedabad, Opposite Air Force Station, Palaj, Gandhinagar, Gujarat 382355, India

ARTICLE INFO

Keywords:
Alzheimer disease
Multi-target directed ligands
Fluorinated triazole-amides/amines
Metal Chelation
ROS scavanging

ABSTRACT

Alzheimer disease is multi-factorial and inflammation plays a major role in the disease progression and severity. Metals and reactive oxygen species (ROS) are the key mediators for inflammatory conditions associated with Alzheimer's. Along multi-factorial nature, major challenge for developing new drug is the ability of the molecule to cross blood brain barrier (BBB). We have designed and synthesized multi-target directed hexafluorocarbinol containing triazoles to inhibit Amyloid β aggregation and simultaneously chelate the excess metals present in the extracellular space and scavenge the ROS thus reduce the inflammatory condition. From the screened compound library, compound **1c** found to be potent and safe. It has demonstrated inhibition of Amyloid β aggregation (IC_{50} of 4.6 μM) through selective binding with Amyloid β at the nucleation site (evidenced from the molecular docking). It also chelate metals (Cu^{+2}, Zn^{+2} and Fe^{+3}) and scavenges ROS significantly. Due to the presence of hexafluorocarbinol moiety in the molecule it may assist to permeate BBB and improve the pharmacokinetic properties. The *in-vitro* results of compound **1c** indicate the promiscuity for the development of hexafluorocarbinol containing triazoles amide scaffold as multi-target directed therapy against Alzheimer disease.

Alzheimer's disease (AD) is a progressive neurodegenerative disorder which involves the degeneration of cholinergic neurons and one of the major causes of dementia in geriatric population.[1] Current treatment of AD restricted to the symptomatic treatments by anticholinesterases (Rivastigmine, Donepezil, Galantamine) and NMDA receptor antagonists Memantine.[2] With growing rate of attrition of drugs in advance stage of clinical trials[3] and limited therapy urged the researchers to discover new drugs towards AD. Histological analysis of the brain dissects of AD patient established the presence of extracellular deposit of peptide Amyloid β plaque,[4] and intracellular neurofibrillary tangle of hyper phosphorylated tau protein.[5] Proteopathy in AD is enhanced by other factors such as oxidative stress and inflammation and metal dyshomeostasis.[6] In normal brain, 0.04 mg/g fresh tissue sample contains iron with concentration of ~ 720 μM and abundantly found in basal ganglia region. Zinc concentration is 10 times higher in brain as compared to the serum and estimated to be around 150 μM, where as the concentration of copper in human frontal lobe and cerebellum is in the range of 60 ~ 110 μM.

As compared to healthy parenchyma in brain, these metals are found 5.7, 2.8, and 3.1 times higher (copper, zinc and iron respectively) and aggravates the aggregation of Amyloid β through binding at *N*-terminus His6, His13 and His14 residue of the peptide.[7] Metals such as Cu (I/II) and Fe (II/III) also produce reactive oxygen species (ROS) which leads to neuronal cell death.[8,9] Clioquinol an analogue of chloroquine, has shown moderate affinity towards metal which shift the entrapped metal towards essential metallo-cycle in brain and currently under phase II clinical trial.[10]

Complex disease which involves multiple pathways needs the

* Corresponding author.
E-mail address: bichismita77@gmail.com (B. Sahu).
[d] Equal contribution.
[e] Current affiliation: Department of Bio-Engineering, Birla Institute of Technology, Mesra, Ranchi, India.

https://doi.org/10.1016/j.bmcl.2021.127999
Received 4 January 2021; Received in revised form 15 March 2021; Accepted 19 March 2021
Available online 9 April 2021

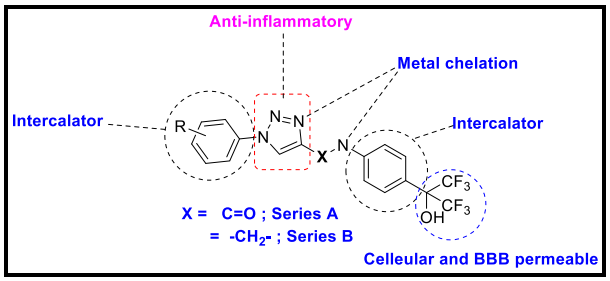

Fig. 1. Designing of the scaffold to target multiple pathways related to AD.

therapeutic strategy which can engage multiple signalling pathways simultaneously. Multi-target directed ligand (MTDL) is a strategy in drug discovery process, where the single molecule is designed with its multiple pharmacophoric properties to engage multiple targets simultaneously.[11] There is a substantial portion of the approved drugs are multi-target-directed drugs for other diseases also.[12]

Amyloid aggregation is the major hallmark for AD and the aggregation process is induced by many biological factors. The hydrophobic core with sequence KLVFF undergoes self aggregation and produce toxic oligomers and plaues.[13] Therefore, controlling amyloid aggregation through those pathways can be effective. Mitochondrial dysfunction and oxidative stress are key players in the pathogenesis of Alzheimer's disease.[14] Aβ species can also induce oxidative stress, by entering into mitochondria and increasing the production of reactive oxygen species (ROS), which, in turn, damage important macromolecules.[15] The Zn^{2+} and Cu^{2+} ions can bind to Aβ and induce further formation of amyloid aggregates.[16,17] Based on the disease molecular mechanism of action, it is postulated molecules which can inhibit Aβ aggregation by blocking the hydrophobic core and exhibit antioxidant/anti-inflammatory properties with metal chelation ability can be a potential therapeutic molecule to treat AD.

The driving force for aggregation of Amyloid beta (Aβ) peptide is the core residue penta-peptide fragment (KLVFF). Moreover, the bis-phenylalanine (FF) dipeptide sequence undergoes self-aggregation to form diverse nano-structures which is now currently utilized in designing novel nano material.[18] Many aromatic compounds including curcumin have found to inhibit Aβ aggregation efficiently and they have common feature of two aromatic rings separated by an optimal linker. Therefore, we have incorporated two aromatic residues in our scaffold, anticipating that aromatic rings may interact with the phenyl alanine residue of KLVFF fragment of Aβ peptide through π-π-interaction and block the aggregation.

Triazoles as potential pharmacophore for the neurodegenerative diseases with anti-inflammatory activity.[19] Triazole based compounds are now under study for the treatment of many neurological disorders such as epilepsy. Di-triazole based compounds have been explored recently as therapeutics for the treatment of Alzheimer's disease.[20] Recently, triazole based compound QTC-4-MeOBnE was selected through virtual screening and shown promising results *in-vivo*.[21] We have selected triazole as part of the scaffold in aniticipation that it may exert anti-inflammatory/anti-oxidant activity and simultaneously can be explored for the metal chelation due to the presence of heteroatom. Therefore, by placing suitable functional group adjacent to 1,2,3 triazole moiety can lead to effective metal chelation. Therefore, triazole amides and triazole methylamines are incorporated as linker, which can hold the two aromatic rings at optimum distance for Aβ interaction and simultaneously chelate the metal and demonstrate anti-oxidant/anti-inflammatory properties (Fig. 1).

Hexafluorocarbinol group is an interesting pharmacophore with hydroxyl group flanked by two CF_3 group and has been explored previously for Aβ inhibition. HFIP (hexaflouroisopropanol) is used as solvent for disaggregating the Aβ peptide and molecules containing this functional moiety are found as bioactive. Therefore, incorporation of hexafluorocarbinol in the molecule may increase the disaggregation properties of molecule and due to the presence of multiple fluorines it may increase the cellular permeability and plasma half-life of the drug.

We have designed two series of compounds (series A, containing triazole amide and series B containing triazole amine) for further synthesis and *in-vitro* evaluations

Molecular docking was performed prior to the synthesis of compounds. The compounds were docked against $Aβ_{42}$ Monomer (PDB ID-1IYT) using Autodock 4.2 software as discussed in detail in the methodology section. The purpose of docking was to investigate whether the compounds acquire the best possible interaction with the monomer particularly with the hydrophobic core bearing the KLVFF sequence (AA 16–20) which is considered to be the self-recognition site. During the nucleation phase, $Aβ_{42}$ monomers aggregate to form the oligomers and then form fibrils via this self-recognition site.

We have performed docking studies with representative compounds from both series (1a from Series A and 2a from Series B). Four different grids are generated and compounds are docked (Table 1).

Representative examples from both the series have demonstrated similar binding affinity with slightly preferential activity towards grid 2 which contain the hydrophobic core fragment KLVFF.

A closer analysis of interaction pattern of 1a and 2a suggested that, the hexafluorocarbinol group present in the compound, exhibits certain specific interactions with the amino acids of the peptide and anchors the compound in such a way that the phenyl ring of the scaffold which interacts with the aggregation prone diphenylalanine FF (Phe19 and 20) motif. Hexafluorocarbinol group plays an important role since without this group, although molecule binds with Aβ, but the aggregation prone diphenyl alanine (FF) remains exposed (Fig. 2). These phenylalanine residues are shown to play a predominant role in the fibril formation and aggregation process through pi-pi stacking type of interactions.[22,23]

These residues when blocked, interactions of one monomer with the other may thus be prevented which will in turn hinder the Aβ aggregation process.

Furthermore, other favorable interactions such as electrostatic, hydrogen bonding and Van der Waals types of interactions are observed.

The difference or change in the intermolecular interactions and binding energy was evaluated with the positional switch of the hexafluorocarbinol (HFC) group. Similar pattern of interactions is observed for the compound 1g (Fig. 4).

In case of 1g, the phenyl group attached to amide was found to be engaged with Phe19 instead of the phenyl attached to triazole. It also retained all the conventional interactions as 1a.

When amide was replaced with methylamine, compound 2a has demonstrated similar interaction with preferential binding at grid 2 and retained favorable interaction with Phe19 (supporting information,

Table 1
Binding energy of compound1a and 2a.

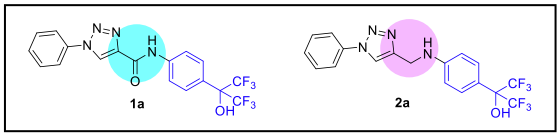

Compound	Grid	Binding Energy (Kcal/mol)
1a	1	−4.12
	2	−4.73
	3	−4.58
	4	−3.41
2a	1	−4.29
	2	−4.69
	3	−3.84
	4	−3.61

Grid 1: AA 1–10; Grid 2: AA 11–21; Grid 3 AA 22–31; Grid 4 AA 32–42.

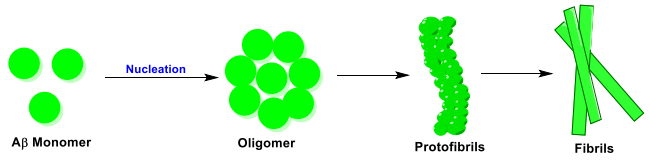

Fig. 2. Process of Amyloid β (Aβ) aggregation. The Aβ monomer aggregates to form oligomer which further aggregates to form fibrils which are highly neuro-toxic.

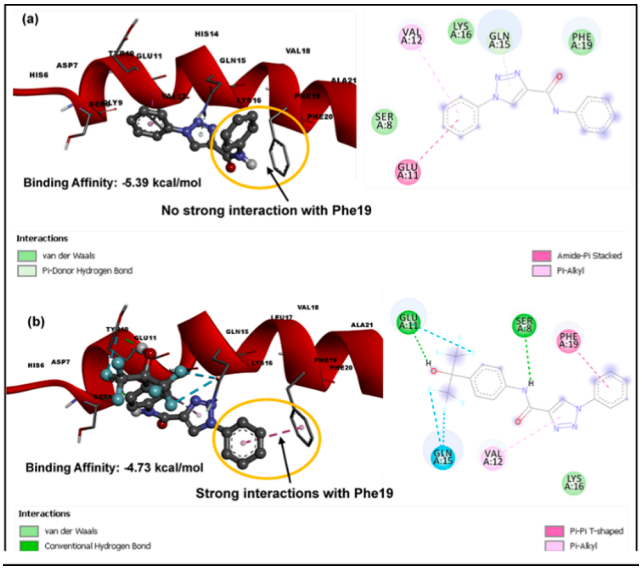

Fig. 3. The intermolecular interactions and binding affinities of (a) Triazole-amide (without Hexafluorocarbinol) and (b) Compound 1a with $A\beta_{42}$ monomer have been depicted. In both the images, the 3D representation is displayed on the left and the 2D representation on the right, whilst the colour code for each interaction being displayed at the bottom. The $A\beta_{42}$ monomer is depicted in ribbon form in red colour while the designed molecules are represented in ball and stick. Interacting residues of $A\beta_{42}$ monomer were displayed in stick representation. Colour key of the atoms represented is as follows: Carbon-Grey, Hydrogen- White, Oxygen- Red, Nitrogen- Blue, and Fluorine- Cyan.

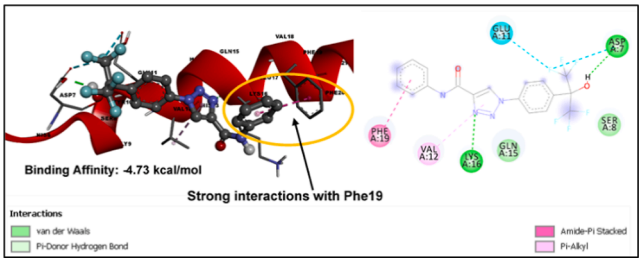

Fig. 4. Intermolecular interactions and binding affinity of Compound 1 g with $A\beta_{42}$ monomer. The positional switch of hexafluorocarbinol group does not predominantly affect the anchoring tendency of the molecule and thus results into similar π-π interaction as observed with Compound 1a (Fig. 3). The colour coding for the atoms is the same as represented in Fig. 3.

Fig. S2).

Therefore, compound library is generated where; phenyl rings have been substituted with electron donating as well as withdrawing groups. To our delight, we have found similar trend in the *in-vitro* $A\beta_{42}$ aggregation inhibition study (Fig. 5) of triazole amides 1c and 1j (positional switch of hexafluorocarbinol group).

Compounds were synthesized by using known synthetic protocols (Scheme 1).[24] For series A, triazole amides (1 a-k) were prepared from

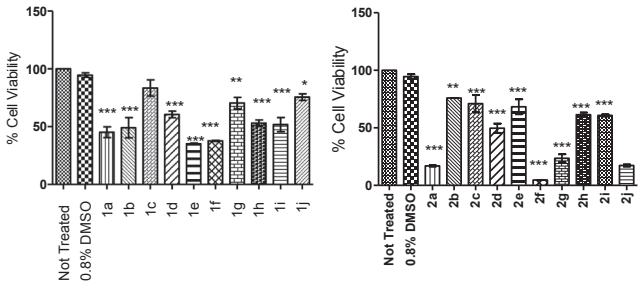

Fig. 5. Cytotoxicity Evaluation: The cytotoxicity of the synthesized compounds (1a-1j and 2a-2j) were evaluated using PC-12 cells. The cells were incubated with the compounds at 40 μM concentrations for 24 h and then the cell viability was evaluated using Alamar Blue reagent. The percentage cell viability after treatment was compared with cells that were not treated.

the coupling of corresponding triazole acids (3) and the aryl amine (4) by using standard coupling reagents such as DCC and HOBt. Triazole acids were obtained from the basic hydrolysis of corresponding triazole esters (5). Triazole esters were in turn prepared via click reaction of aryl azides (6) and ethyl propiolate (7). All the synthesized compounds (1 a-k) were isolated in moderate to good yield.

Table 2
Synthetic scheme and structures of the compounds from series A &B.

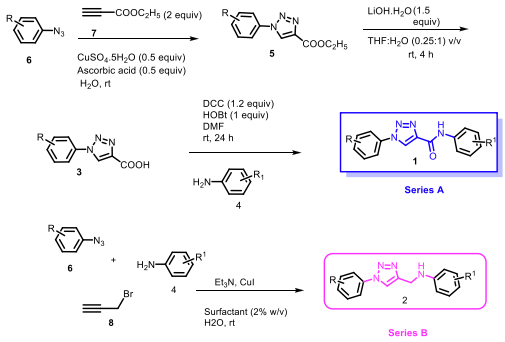

Compound	Structure	Compound	Structure
1a	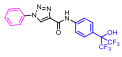	2a	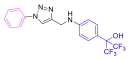
1b	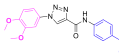	2b	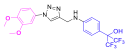
1c	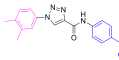	2c	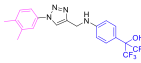
1d	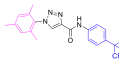	2d	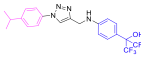
1e	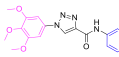	2e	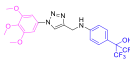
1f	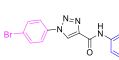	2f	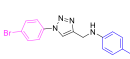
1g	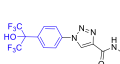	2g	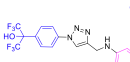
1h	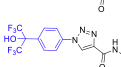	2h	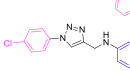
1i	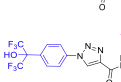	2i	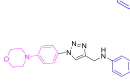
1j	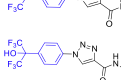	2j	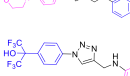

Similarly, series B triazole amines were synthesized via one pot reaction of aryl azide (6), propargyl bromide (8) and corresponding aryl amines (4) in water in the presence of copper iodide, triethylamine and surfactant. Although, a step-wise synthesis was tried by utilizing the click reaction of arylazide with propargyl bromide (9) followed by condensation with arylamine in the presence of base, we have failed to isolate the intermediate. One pot reaction of arylamine, aryl azide and propargyl bromide in water in the presence of catalyst copper iodide and base triethylamine also failed to yield any desired product.[25] Surfactants are known to enhance the reaction rate, therefore we have screened surfactants (SDS and DOSS) in water for above mentioned reaction. Reactions were preceded well and all triazole amines (2a-i) were isolated in moderate yields. Synthesized compounds are summarized in Table 2. Compounds were characterized by ^{1}H, ^{13}C NMR and HRMS. Presences of fluorine were confirmed by ^{19}F NMR.

Prior to performing Aβ binding assay, we have screened the compounds for their cytotoxicity against neuronal cell (PC-12) since, the main limitation for the lead compounds in the discovery and development process is their intolerable toxicity profile. The toxic effects of the synthesized compounds were evaluated against PC12 neuronal cell line at a single concentration of 40 μM using Alamar Blue reagent. The results (Fig. 5) indicate that a fair number of compounds posed cell viability >60% in PC12 cells at the employed concentrations.

We observed that when hexafluorocarbinol is incorporated at the right-hand aromatic ring compound (1g) was found to be less toxic as compared to the left-handed hexafluourocarbinol substituted counterpart (1a). Left-handed hexafluorocarbinol substituted compounds with polar group substitutions (OMe, Cl, Br) in right-hand aromatic ring or replacement of aromatic ring with heteroaromatic ring were cytotoxic for triazole amides. Only 3, 4 dimethyl substitutions on either of the aromatic ring (1j, 1c) were found to be safer for further *in-vitro* evaluation and cytotoxicity did not altered much by positional switch of hexafluorocarbinol group. Switching the linker from triazole amide (1a) to triazole methylamine (2a), found to be toxic. Substitutions such as 3,4 dimethoxy, 3,4 dimethyl and 3,4, 5 trimethoxy in left-hand aromatic ring found to possess good cell viability as compared to halo substitutions. However, unlike the 3,4 dimethyl substituted amides (1j and 1c), positional switch of hexafluorocarbinol groups from left hand aromatic ring to right hand resulted considerable cytotoxicity.

Compounds which have demonstrated good cell viability (less toxic) were selected and screened for their ability to bind with Aβ monomer

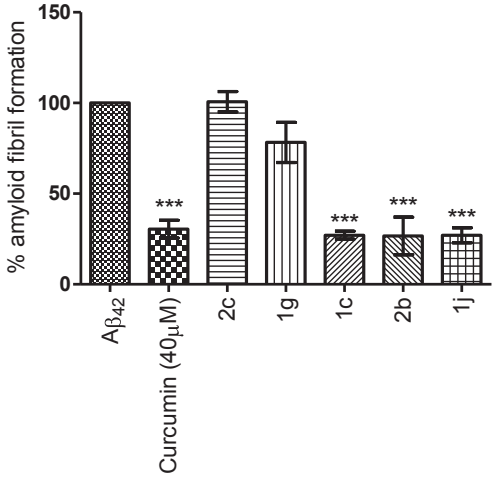

Fig. 6. Amyloid beta fibrillation formation: The compounds were incubated with $A\beta_{42}$ (10 μM) at 40 μM concentration and for 24 h (at 37 °C) and the percentage of $A\beta_{42}$ fibrillation formation was calculated using Thioflavin T reagent. The statistical significance was evaluated using Dunnet test, and compared with amyloid beta 42 kept for fibrillation for 24 h. (*** means n = 3, $p < 0.05$).

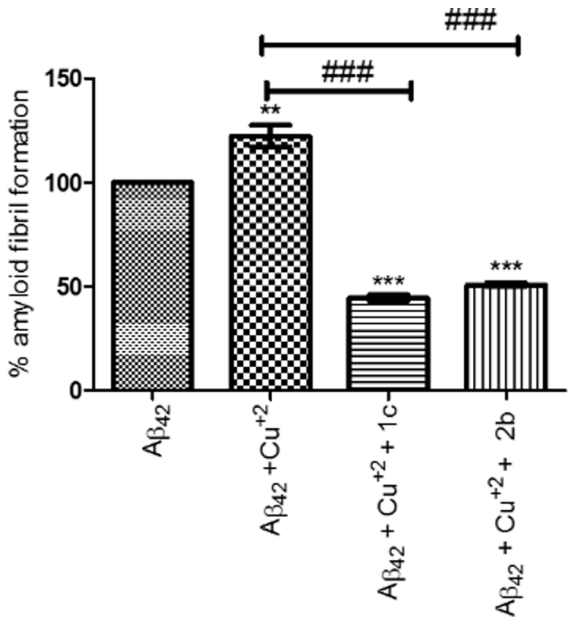

Fig. 7. Copper Chelating Effect: The compounds were incubated with $A\beta_{42}$ (10 μM) with 10 μM Cu^{+2} concentration for 24 h (at 37 °C, 180 rpm) and the percentage of $A\beta_{42}$ fibrillation formation was calculated using Thioflavin T reagent. The statistical significance was evaluated using Dunnet test, and compared with $A\beta_{42}$ kept for fibrillation for 24 h. (n = 3, *** vs $A\beta_{42}$ alone, ### means vs $A\beta_{42}$ + Cu^{+2}).

and inhibit aggregation following standard Thioflavin T assay protocol. We have selected compound 1 g, 1c and 1j from triazole amides to screen for their ability to inhibit $A\beta_{42}$ aggregation. Compound 1g failed to inhibit $A\beta_{42}$ aggregation. However, dimethyl substitution at either aromatic ring (1c and 1j) leads to effective inhibition of aggregation at the concentration of 40 μM. The inhibition was comparable to that of curcumin at the (Fig. 6). Compounds with 3,4 dimethyl substitution (2c) and 3,4 dimethoxy substitution (2b) at one of the aryl group were selected from the triazole methylamine scaffold. To our surprise, compound with 3,4 dimethyl substitution (2c) failed to inhibit aggregation (Fig. 6). However, dimethoxy substituted triazole amine (2b) demonstrated similar inhibition as of compound 1c.

Presence of metals such as Zn, Cu and Fe are known to accelerate the aggregation rate of Aβ. Therefore, to find a potent compound which can

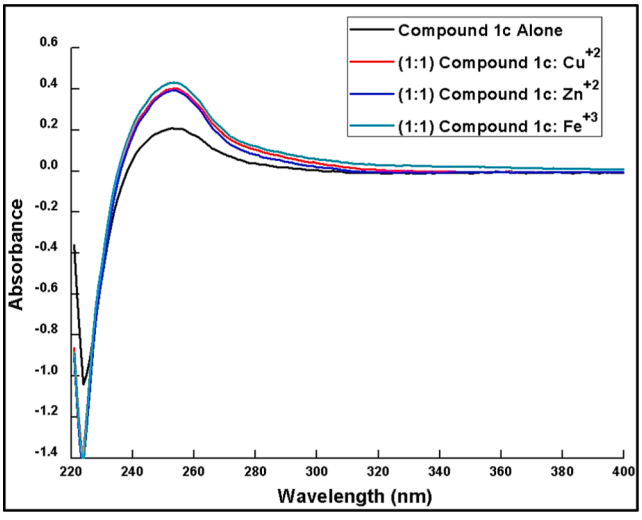

Fig. 8. Metal chelation of compound 1c; The UV–Vis spectra of compound 1c incubated with Cu^{+2}, Zn^{+2} and Fe^{+3}.

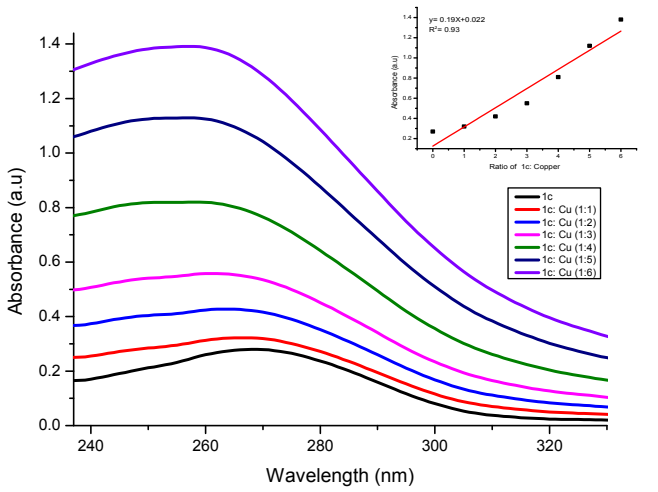

Fig. 9. UV–vis spectra of compound 1c at different ratio of Cu^{+2} in HEPES buffer at room temperature.

inhibit $A\beta_{42}$ aggregation, we have decided to screen the hit compounds from both series (1c and 2b) and tested for their ability to inhibit Aβ aggregation in the presence of metal such as copper (Fig. 7).

Amount of aggregation found to be more in the presence of copper without any compounds (Fig. 7). Compounds from both series were found to reduce the aggregation up to 50% in the presence of copper. To our observation, triazole amide 1c was found to inhibit aggregation slightly better than the triazole amine 2b. Although, 1c and 2b are found to be equipotent, amides are metabolically stable than amines. Therefore, we have anticipated that 1c can be consider as scaffold of choice and potent molecules can be further generated by doing systematic structure–activity-relationship (SAR) study. Therefore, compound 1c was envisaged as the potent hit molecule from the present screenings and the IC_{50} for $A\beta_{42}$ fibril formation inhibition was determined to be 4.6 ÂμM (graph presented in supporting info as Fig. S61).

Metals play very important role in pathophysiology of AD and the interaction of Aβ and biological relevant metals such as copper, zinc, iron has already proven the formation of highly toxic aggregated complex from Aβ. Therefore, many compounds with metal chelating ability such as Desferroxamine (DFO), DP-109, Clioquinol etc., have been evaluated and they have demonstrated success in animal model (Fig. 8).

Therefore, we have evaluated the hit compound 1c for its ability to chelate metals such as copper, zinc and iron. Compound 1c

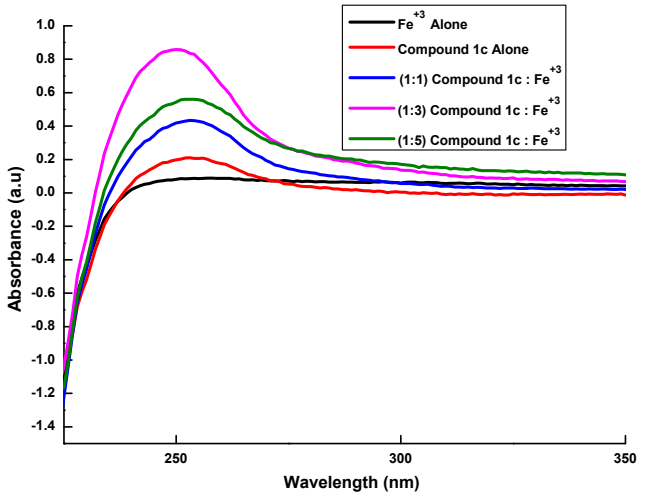

Fig. 10. UV–vis spectra of compound 1c at different ratio of Fe^{+3} in HEPES buffer at room temperature.

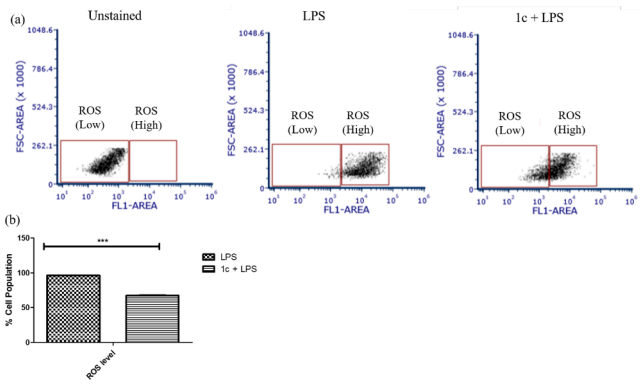

Fig. 11. ROS scavenging effect of 1c compound: compound 1c ROS scavenging effect was analysed using DCFDA analysis, after LPS inflamed PC-12 cells treatment with 1c compound (40 μM) after 24 h a) FACS analysis dot blot showing cell population percentage (ROS (low) vs ROS (High)) b) Bar graph of FACS dot blot ROS level after 1c compound treatment (n = 3, *** $p < 0.001$).

demonstrated absorption maximum around 255 nm. When incubated with the compound in 1:1 ratio with $CuSO_4$, Zn SO_4 and $FeCl_3$ at 50 μM concentration for 30 min (in HEPES buffer at pH 7.4, at room temperature) a significant hyperchromic shift observed for all the metals. The change in the intensity of the sample in the presence of metal ion confirms the interaction of the compound. To confirm further, we have titrated the compound 1c with copper salts of varying ratio (1c: M = 1:0, 1: 1, 1:2, 1:3. 1:4. 1:5 and 1:6). The absorbance of the compound increased in proportion of the salt which confirms the binding (Fig. 9).

When the binding study was performed with Zn^{+2} and Fe^{+3}, increase in absorbance obtained for Fe^{+3} with increment of concentrations was observed as in case of Cu^{+2} (Fig. 10). However, minimal effects for increase in concentration observed for Zn^{+2} (data not shown).

Reactive oxygen species (ROS) involved in initiation and progression of many inflammatory path-way. In AD, metal mediated redox reactions produce many ROS which may contribute to neuronal cell damage and death. Apart from metal chelation, 1,2,3 triazoles are privileged heterocyclic core with many interesting biological activities. Their stability towards acidic/basic hydrolysis, high dipole moment (~5 D), ability of the moiety to interact with biological target through hydrogen bonding, dipole–dipole interaction, π-π stacking make them very attractive for medicinal chemist to design new scaffolds. Compounds possessing these scaffolds are known to exhibit anti-inflammatory properties through inhibition of ROS production. Therefore, we have investigated the efficacy of the hit molecule 1c to scavenge ROS production in cell. Inflammation was induced in PC12 cell through LPS (liposaccharide) and cells are incubated in the presence of compound 1c at the concentration of 40 μM as explained in methodology section. The efficiency to scavenge ROS was evaluated using FACS (Fig. 11). The analysis was done using DCFDA reagent. Initially, desired PC-12 cells population was selected by applying gate in FSC area vs SSC area graph in unstained cell populations. Thereafter, only singlet cells population was selected by plotting and gating desired population in FSC area vs FSC height population. Propidium iodide (PI) staining was used to eliminate dead cells population from the FACS study, and live cells were taken in to the account for ROS activity. The DCFDA positive live cells population was further evaluated plotting a dot blot (FL1 area vs FSC area) and applying a quadrant to the population. The cell population shown in Fig. 6a demonstrate ROS^{high} demonstrating the high fluorescence in PC-12 cells due to DCFDA. The fluorescence intensity of DCFDA is directly proportional to the ROS level, and hence can be used to distinguish ROS activity in the cells. The percentage of DCFDA ROS^{high} population in LPS (10 μg/mL) treated was much higher as compare to the PC-12 cells treated with 1c compound (40 μM). This shows that there is a significant reduction in ROS levels after incubating the cells with 1c compound

(Fig. 11b)

Involvement of multiple pathological factors including Aβ aggregation, Aβ-metal interaction, reactive oxygen species, and inflammation makes AD very complex and pose a great challenge in disease understanding. Therefore, targeting multiple pathways simultaneously through a single molecule seems to be very attractive. We have rationally designed triazole amide scaffold to target Aβ aggregation, metal chelation and inflammation. Compound 1c found to effectively inhibit Aβ aggregation even in the presence of copper. It also demonstrated its ability to chelate the metal and possess good anti-oxidant activity. Due to the presence of multiple fluorine our hit molecule 1c, we speculate that it may cross the BBB. Therefore, the designed scaffold (triazole amide) may serve as the scaffold of choice for further SAR development which may provide a potent multi-target directed ligand based drug molecule for the treatment of AD.

Declaration of Competing Interest

The authors declare that they have no known competing financial interests or personal relationships that could have appeared to influence the work reported in this paper.

Acknowledgments

Authors are thankful to Prof. Kiran Kalia, Director, National Institute of Pharmaceutical Education and Research (NIPER)-Ahmedabad and Department of Pharmaceuticals, Ministry of Chemicals and Fertilizers, Govt. of India for giving support as student fellowships and required facilities to complete this work.

Appendix A. Supplementary data

Supplementary data to this article can be found online at https://doi.org/10.1016/j.bmcl.2021.127999.

References

1 (a)2017 Alzheimer's Disease Facts and Figures. Alzheimer's Dement. 2017, 13 (4), 325–373.(b) Hardy JA, Higgins GA. Alzheimer's disease. *Science*. 1992:184–185. (c) Jonsson T, Atwal JK, Steinberg S, et al. A mutation in APP protects against Alzheimer's disease and age-related cognitive decline. *Nature*. 2012;488:96.
2 Yiannopoulou KG, Papageorgiou SG, Ther Adv Neurol Disord 2013, 6, 19–33; (b) Cummings J, Lee G, Ritter A, et al. Alzheimer's Dement Transl Res Clin Interv 2020, 6; 1-29.
3 Cummings JL, Morstorf T, Zhong K, Alzheimer's Res Ther 2014, 6, 37; (b) Mullane K, Williams M, Biochemical Pharmacology. Elsevier Inc. February 1, 2013, 289–305.
4 Tanzi RE, Bertram L, Cell. Cell Press February 25, 2005, 545–555; (b) Hillen H, Front Neurosci 2019, 13, 1154.
5 (a) Lindsley CW, Hooker JM. *ACS Chem Neurosci*. 2018;21:2519.(b) Pickett EK, Herrmann AG, Mc Queen J, et al. *Cell Rep*. 2019;29(11):3592–3604.
6 (a) Hull M, Lieb K, Fiebich B. *Curr Med Chem*. 2002;9:83–88.(b) Ray B, Lahiri DK. *Curr Opin Pharmacol*. 2009:434–444.(c) Lue LF, Kuo YM, Beach T, Walker DG. *Mol Neurobiol*. 2010;41:115–128.(d) Lue L-F, Brachova L, Civin HW, Rogers J. *J Neuropathol Exp Neurol*. 1996;55:1083–1088.
7 (a) Adlard PA, Bush AI. *J Alzheimers Dis*. 2006:145–163.(b) Myhre O, Utkilen H, Duale N, Brunborg G, Hofer T. *Oxid Med Cell Longevity*. 2013:1–19.(c) Adlard PA, Bush AI. *J Alzheimers Dis*. 2018:1369–1379.(d) Cristóvão JS, Santos R, Gomes CM. *Oxid Med Cell Longevity*. 2016:1–13.(e) Wang L, Yin YL, Liu XZ, et al. *Z. Transl Neurodegener*. 2020;9:10.(f) Liu Y, Nguyen M, Robert A, Meunier B. *Acc Chem Res*. 2019;52:2026–2035.
8 (a) Duce JA, Bush A. *I Progr Neurobiol*. 2010:1–18.(b) Schrag M, Mueller C, Zabel M, et al. *Neurobiol Dis*. 2013;59:100–110.(c) Sun L, Sharma AK, Han BH, Mirica LM. *ACS Chem Neurosci*. 2020;11:2741–2752.(d) Bush AI, Pettingell WH, Multhaup G, et al. *Rapid Science (80)*. 1994;265:1464–1467.(e) Opazo C, Inés Barría M, Ruiz FH, Inestrosa N. *C. BioMetals*. 2003;16:91–98.(f) Rana M, Sharma AK. *Cu and Zn Metallomics*. 2019:64–84.(g) Faller P, Hureau C. *Dalton Trans*. 2009;7: 1080–1094.
9 (a) Zhu X, Su B, Wang X, Smith MA, Perry G. *Cell Mol Life Sci*. 2007:2202–2210.(b) Cheignon C, Tomas M, Bonnefont-Rousselot D, Faller P, Hureau C, Collin F. *Redox Biol*. 2018:450–464.(c) Tönnies E, Trushina E. *J Alzheimers Dis*. 2017:1105–1121. (d) Hureau C, Faller P. *Biochimie*. 2009:1212–1217.
10 (a) Bareggi SR, Cornelli U. *CNS Neurosci Ther*. 2012:41–46.(b) Di Vaira M, Bazzicalupi C, Orioli P, Messori L, Bruni B, Zatta P. *Inorg Chem*. 2004;43:3795–3797.
11 (a) Zhou J, Jiang X, He S, et al. *J Med Chem*. 2019;62:8881–8914.(b) Medina-Franco JL, Giulianotti MA, Welmaker GS, Houghten RA. *Drug Discovery Today*. 2013: 495–501.(c) Morphy R, Kay C, Rankovic Z. *Drug Discovery Today*. 2004:641–651.
12 (a) Cavalli A, Bolognesi ML, Mînarini A, et al. Multi-target-directed ligands to combat neurodegenerative diseases. *J Med Chem*. 2008:347–372.(b) Van Der Schyf CJ. The use of multi-target drugs in the treatment of neurodegenerative diseases. *Expert Rev Clin Pharmacol*. 2011:293–298.(c) Rochais C, Lecoutey C, Gaven F, et al. *J Med Chem*. 2015;58:3172–3187.(d) Jiang XY, Chen TK, Zhou JT, et al. *ACS Med Chem Lett*. 2018;9:171–176.(e)Prati F, Bottegoni G, Bolognesi ML, Cavalli J Med Chem 2018, 619–637.(f) Basha SJ, Mohan P, Yeggoni DP, et al. *Mol Pharm*. 2018;15:2206–2223.(g) Bolognesi ML, Cavalli A, Valgimigli L, et al. *J Med Chem*. 2007;50:6446–6449.
13 (a) Lowe TL, Strzelec A, Kiessling LL, Murphy RM, Biochemistry 2001, 40 (26), 7882–7889; (b) Enache TA, Chiorcea-Paquim AM, Oliveira-Brett AM, Anal. Chem. 2018, 90 (3), 2285–2292.
14 (a) Han X, He G. *ACS Chem Neurosci*. 2018;21:198–210.(b) Guo CY, Sun L, Chen XP, Zhang DS. *Neural Regen Res*. 2013;8:2003–2014.(c) Cha MY, Han SH, Son SM, et al. *PLoS ONE*. 2012;7:4.(d) Panza F, Lozupone M, Logroscino G, Imbimbo BP. *Nat Rev Neurol*. 2019:73–88.(e) Mawuenyega KG, Sigurdson W, Ovod V, et al. *Science (80)*. 2010;330:1774.(f) Yang LB, Lindholm K, Yan R, et al. *Nat Med*. 2003;1:3–4.
15 Auten RL, Davis JM. *Pediatr Res*. 2009:121–127.
16 (a) Ha C, Ryu J, Chan BP. *Biochemistry*. 2007;46:6118–6125.(b) Kim A, Lim S, Kim Y. *Int J Mol Sci*. 2018;19:128.
17 (a) Rana M, Sharma AK. *Metallomics*.. 2019:64–84.(b) Liu H, Qu Y, Wang X. *Future Med Chem*. 2018:697–701.
18 (a) Acuña SM, Veloso MC, Toledo PG. *J Nanomater*. 2018:2018.(b) Panda JJ, Chauhan VS. *Polym Chem*. 2014:4418–4436.
19 (a) Fischer C, Zultanski SL, Zhou H, et al. *Bioorg Med Chem. Lett*. 2011;21: 4083–4087.(b) Dheer D, Singh V, Shankar R. *Bioorg Chem*. 2017:30–54.(c) Xu J-H, Fan Y-L, Zhou J. *J Heterocycl Chem*. 2018;55(8):1854–1862.(d) Ferreira VF, Da Rocha DR, Da Silva FC, Ferreira PG, Boechat NA, Magalhães JL. *Expert Opin Ther Pat*. 2013:319–331.
20 (a) Rastegari A, Nadri H, Mahdavi M, et al. *Bioorg. Chem*. 2019;83:391–401.(b) Jones MR, Dyrager C, Hoarau M, et al. *J. Inorg. Biochem*. 2016;158:131–138.(c) Di Pietro O, Alencar N, Esteban G, et al. *Bioorganic Med Chem*. 2016;24:4835–4854.(d) Li JC, Zhang J, Rodrigues MC, et al. *Bioorganic Med Chem Lett*. 2016;26:3881–3885. (e) Dyrager C, Vieira RP, Nyström S, Nilsson KPR, Storr T. *New J Chem*. 2017;41: 1566–1573.(f)Jones MR, Service EL, Thompson JR, et al. Metallomics 2012, 4 (9), 910–920.(g) Kaur A, Mann S, Kaur A, et al. *Bioorg. Chem*. 2019;87:572–584.
21 Fronza MG, Baldinotti R, Martins MC et al. Sci Rep 2019, 9, 1–14.
22 Gazit EA. *FASEB J*. 2002;16:77–83.
23 Cukalevski R, Boland B, Frohm B, Thulin E, Walsh D, Linse S, ACS Chem Neurosci 2012, 3, 1008–1016.
24 Due-Hansen ME, Pandey SK, Christiansen E, Andersen R, Hansen SVF, Ulven T. *Org. Biomol. Chem*. 2016;14(2):430–433.
25 Yan ZY, Zhao Y, Bin, Fan MJ, Liu WM, Liang YM, Tetrahedron 2005, 61, 9331–9337.
26 Goodsell DS, Zardecki C, Di Costanzo L, et al. *Protein Sci*. 2020;29:52–65.
27 Crescenzi O, Tomaselli S, Guerrini R, et al. *Eur J Biochem*. 2002;269:5642–5648.
28 Morris GM, Huey R, Lindstrom W, et al. *J Comput Chem*. 2009;30:2785–2791.
29 O'Boyle NM, Banck M, James CA, Morley C, Vandermeersch T, Hutchison GR. Open Babel. *J. Cheminform*. 2011;3:1–14.
30 BIOVIA. Dassault Systèmes, Discovery Studio Visualizer, v19.1.0: San Diego, Dassault Systèmes 2019.
31 Zhang S, Duangjan C, Tencomnao T, Liu J, Lin J, Wink M. *Food Funct*. 2020;11: 8179–8192.